Journal of Molecular Structure 1246 (2021) 131208

Contents lists available at ScienceDirect

Journal of Molecular Structure

journal homepage: www.elsevier.com/locate/molstr

Sustainable synthesis of silver nanoparticles using *Alstonia scholaris* for enhanced catalytic degradation of methylene blue

Rajamanickam Rajasekar[a,1], Michael Samuel[a,1], Thomas Nesakumar Jebakumar Immanuel Edison[b,1], Natarajan Raman[a,*]

[a] Research Department of Chemistry, VHNSN College (Autonomous), Virudhunagar – 626 001, Virudhunagar District, Tamil Nadu, India
[b] School of Chemical Engineering, Yeungnam University, Gyeongsan, Gyeongbuk, 38541, South Korea

ARTICLE INFO

Article history:
Received 21 June 2021
Revised 20 July 2021
Accepted 28 July 2021
Available online 29 July 2021

Keywords:
Alstonia scholaris
Silver nanoparticles
Catalyst
Methylene blue
Degradation

ABSTRACT

The present work described a simple, green, and fast approach for the synthesis of silver nanoparticles using an aqueous fruit extract of *Alstonia scholaris*(AS-AgNPs). The role of plant extract was identified as both reducing as well as capping agent in the synthesis of AS-AgNPs. The formation of AS-AgNPs was confirmed through the visible color change from pale yellow to brown and the respective surface plasmon resonance (SPR) peak observed at 426 nm in the UV-Visible (UV-Vis) spectrum. Further, the synthesized AS-AgNPs were characterized using X-ray diffraction (XRD), Fourier transform infrared spectroscopy (FT-IR), Scanning electron microscopy with Energy dispersive spectrum (SEM with EDS), High resolution transmission electron microscopy (HR-TEM), and Dynamic light scattering (DLS) with Zeta potential. The DLS derived average particle size and poly dispersion index (PDI) of AS-AgNPs are about 50 nm and 0.664 with Zeta potential of -22.4 mV, suggested the presence of mono and polydispersive AS-AgNPs with good stability. The synthesized AS-AgNPs were mainly distributed (56 %) as a quasi-spherical shape with size ranges from 5 to 50 nm revealed by SEM and TEM images. Moreover, the catalytic reduction of methylene blue (MB) by AS-AgNPs has been accessed *via* time-dependent UV-Vis spectroscopy. The UV-Vis results suggested that AS-AgNPs show enhanced catalytic activity on the reduction of MB by aqueous sodium borohydride with pseudo first-order kinetics and the calculated rate constant was about 0.7×10^{-3} s^{-1}. Overall, the green synthesized AS-AgNPs have a great catalytic potential in the degradation of MB in water.

1. Introduction

In recent decades the application of metal nanoparticles is vast especially in the field of catalysis, biosensors, medicines, biotechnology, and agriculture [1–5]. Particularly, silver nanoparticles (AgNPs) are desired as a better candidate for environmental applications such as catalytic dye degradation, antibacterial activity, and optical sensors owing to their size and shape-dependent optical, chemical, and electronic properties. Hence, the researchers are mainly focused on the bulk production of AgNPs [6,7]. The chemical reduction of Ag^{+} is one of the simplest ways for the bulk synthesis of colloidal AgNPs. This method has several advantages including easy, fast, and facile fabrication of different dimensions of AgNPs, thereby controlling the physical/chemical properties of resultant materials. Generally, the colloidal AgNPs are synthesized by the addition of external reducing and capping agents [8–11]. Reduction of silver ions using environmentally benign plant extracts, fruit juices, biopolymers, bacteria, and biomass wastes are proved as a better alternative to the commercial reducing/capping agents *viz*., sodium borohydride, ethylene glycol, and hydrazine in terms of environmental and economic aspects [12–14]. The major phytoconstituents present in the bio-sources are responsible for the reduction and protection of synthesized AgNPs. *Alstonia scholaris* (*A. scholaris*) is known as a devil/blackboard tree and a family member of Apocynaceae, native to Asia [15]. Almost all the plant parts of *A. scholaris* have been consumed for the treatment of diarrhea, fever, and ulcers in ancient Siddha and Ayurveda systems. The fruits of *A. scholaris* (Fig. 1) are very lengthy and mainly contain monoterpenoid indole alkaloids and aldehydes which could act as a good reducing agent [16–17].

Water pollution is a serious environmental problem throughout the globe, which occurs mainly due to the discharging of untreated dye effluents from textile industries [18–19]. The accumulation of untreated dye effluents in water bodies can cause serious health

* Corresponding author.
E-mail address: ramchem1964@gmail.com (N. Raman).
[1] Authors contributed equally to this work

https://doi.org/10.1016/j.molstruc.2021.131208
0022-2860/

Fig. 1. Photographic image of *A. scholaris* fruit.

issues to human beings and all living things due to the high chemical oxygen demand. Methylene blue (MB) is one of the important cationic dyes mainly used for the dyeing process in textile industries [20]. Due to the high water solubility, MB is present in the dye effluents of textile industries. Thus the reduction/degradation, removal, and decolorization of MB are scientifically important in terms of environmental concern. The AgNPs assisted catalytic reduction of MB by aqueous sodium borohydride is one of the simple and cost-effective approaches than other existing methods [21–23].

This present work describes a simple, facile, and green synthesis of AgNPs using an aqueous extract of *A. scholaris* fruit, which is termed as AS-AgNPs. The formation of AS-AgNPs is monitored by a visible color change and UV-Vis spectroscopy. Moreover, the synthesized AS-AgNPs are characterized using common analytical methods. Further, the AS-AgNPs have been utilized as a catalyst for the reduction of MB using aqueous $NaBH_4$ and the corresponding reaction kinetics is also studied by UV-Vis spectroscopy.

2. Materials and methods

2.1. Materials

A. scholaris fruits were obtained from Virudhunagar area of Tamil Nadu, India in January 2020. The silver nitrate (purity of 99 %), $NaBH_4$, and MB were purchased from Sigma Aldrich, India, and used without further purification. The Millipore water was consumed for the preparation of *A. scholaris* fruit extract and standard solutions throughout the experiment.

2.2. Preparation of A. scholaris fruit extract

The procured *A.scholaris* fruit was rinsed with Millipore water and chopped into small pieces. 20 g of cleaned fruit was mixed with 100 mL of Millipore water and heated to 80°C for 30 min. The resultant extract was cooled to room temperature and filtered using Whatmann No. 1 paper, the filtrate was further used for the synthesis of AgNPs.

2.3. Synthesis of AS-AgNPs

For the synthesis of AS-AgNPs, 1, 2, 3, 4, and 5 mL of *A.scholaris* fruit extract was mixed with 99, 98, 97, 96, and 95 mL of 0.01 M $AgNO_3$, respectively. After the addition of the extracts, the instant color change was noticed from pale yellow to slightly brown, which indicated the formation of AgNPs. Further, the solutions were allowed to 6 h at room temperature for the total reduction of Ag^+ ions. The synthesized AS-AgNPs were further characterized and utilized as a catalyst.

2.4. Characterization of AS-AgNPs

The formation of AS-AgNPs and catalytic degradation experiments were monitored using Shimadzu UV-1800 model UV-Vis spectrophotometer. The responsible functional groups for the reduction and protection of AS-AgNPs were studied using IRAffinity-1S Fourier Transform Infrared Spectrophotometer. The phase and crystallinity of AS-AgNPs were opened by Bruker D8 Advance X-ray diffractometer. The average particle size and zeta potential of synthesized AS-AgNPs were tested through Nanotrac Wave particle size Zeta potential analyzer. The surface morphologies of AS-AgNPs were examined by VEGA3-TESCAN scanning electron microscopy coupled with Energy Dispersive X-ray Spectrometer (EDS- Bruker, Nano GMBH X' Flash Detector, 5010 model, Germany). The shape and structure of AS-AgNPs were studied by FEI-Tecnai, G2 20 Twin high-resolution transmission electron microscopy.

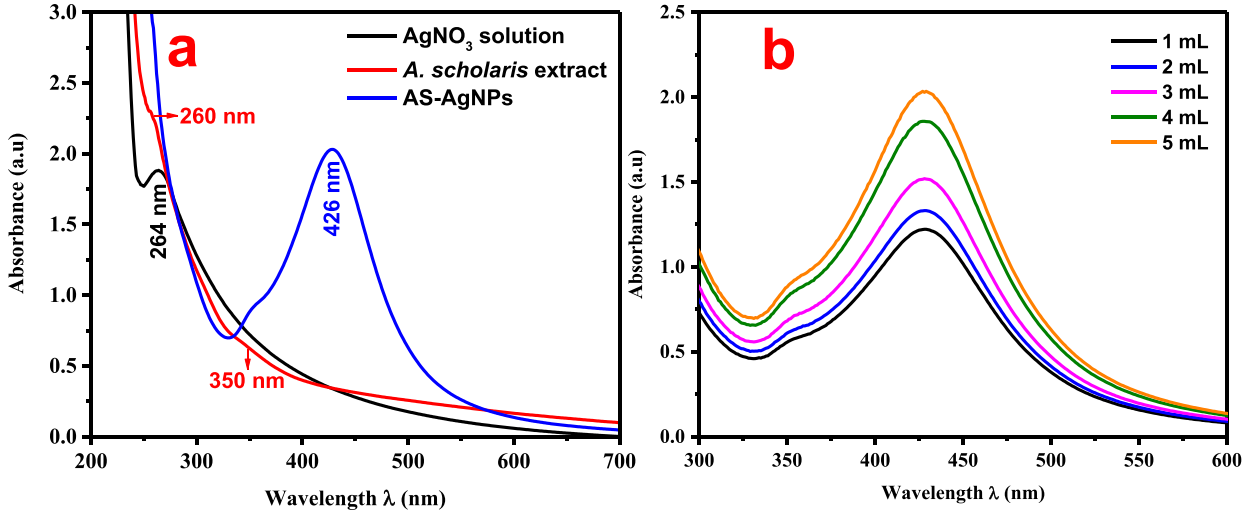

Fig. 2. a) UV-Vis spectra of *A. scholaris* fruit extract and synthesized AS-AgNPs (5 mL); **b)** Effect of concentration of *A. scholaris* fruit extract on synthesis of AS-AgNPs.

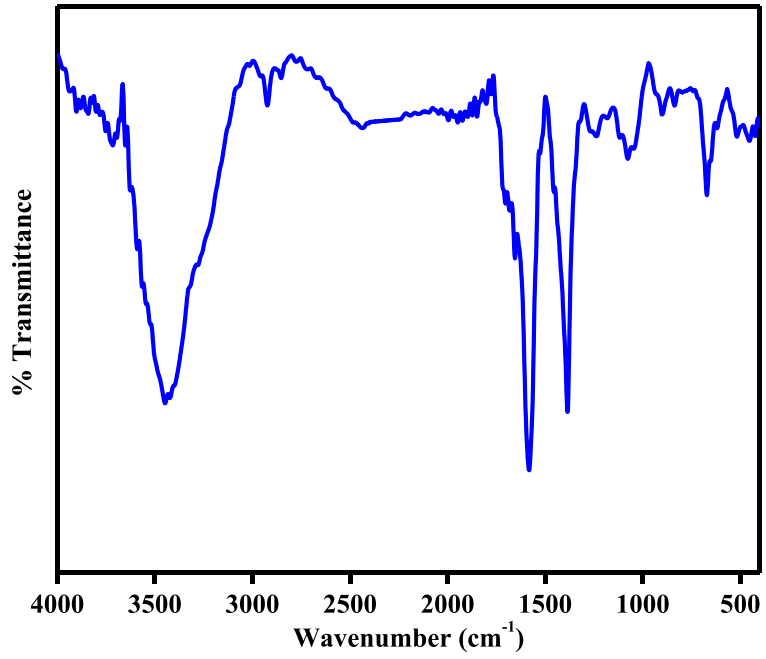

Fig. 3. FT-IR spectrum of synthesized AS-AgNPs.

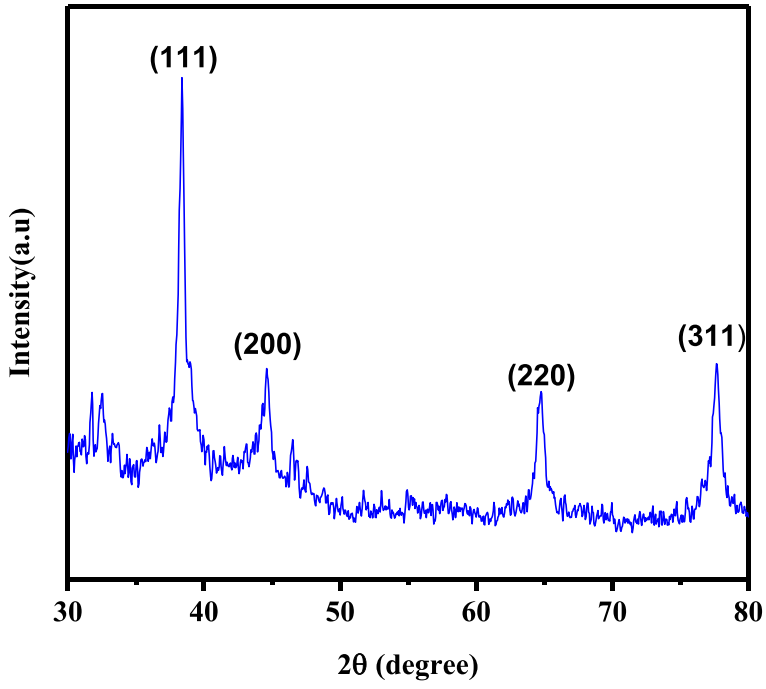

Fig. 4. XRD pattern of synthesized AS-AgNPs.

2.5. Catalytic degradation of MB

The catalytic degradation efficiency of AS-AgNPs was tested against MB dye using $NaBH_4$ as a reducing agent. The degradation experiment was carried out in a standard UV quartzcell cuvette (path length = 1 cm and volume capacity = 4 mL), where 2 mL (100 μM) of MB, 0.95vmL (100 mM) of $NaBH_4$ aqueous solution were mixed with 0.05 mL of AS-AgNPs. The reduction reaction was monitored by measuring the time-dependent absorbance of MB using a UV-Vis spectrophotometer.

3. Results and discussion

3.1. UV–Vis spectroscopy

The formation of AS-AgNPs is visually confirmed through the color change of the solution from pale yellow to dark brown due to the interaction of conduction band electrons and the electromagnetic radiation commonly known as surface plasmon resonance (SPR) [24]. The respective SPR absorption peak can be easily recognized by UV-Vis spectroscopy, therefore this technique is one of

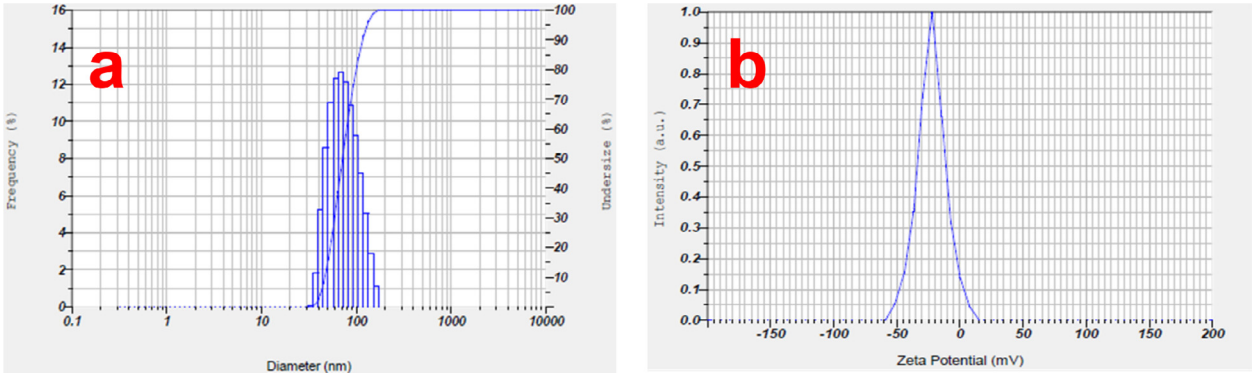

Fig. 5. **a)** DLS size distribution of AS-AgNPs; **b)** Zeta potential spectrum of synthesized AS-AgNPs.

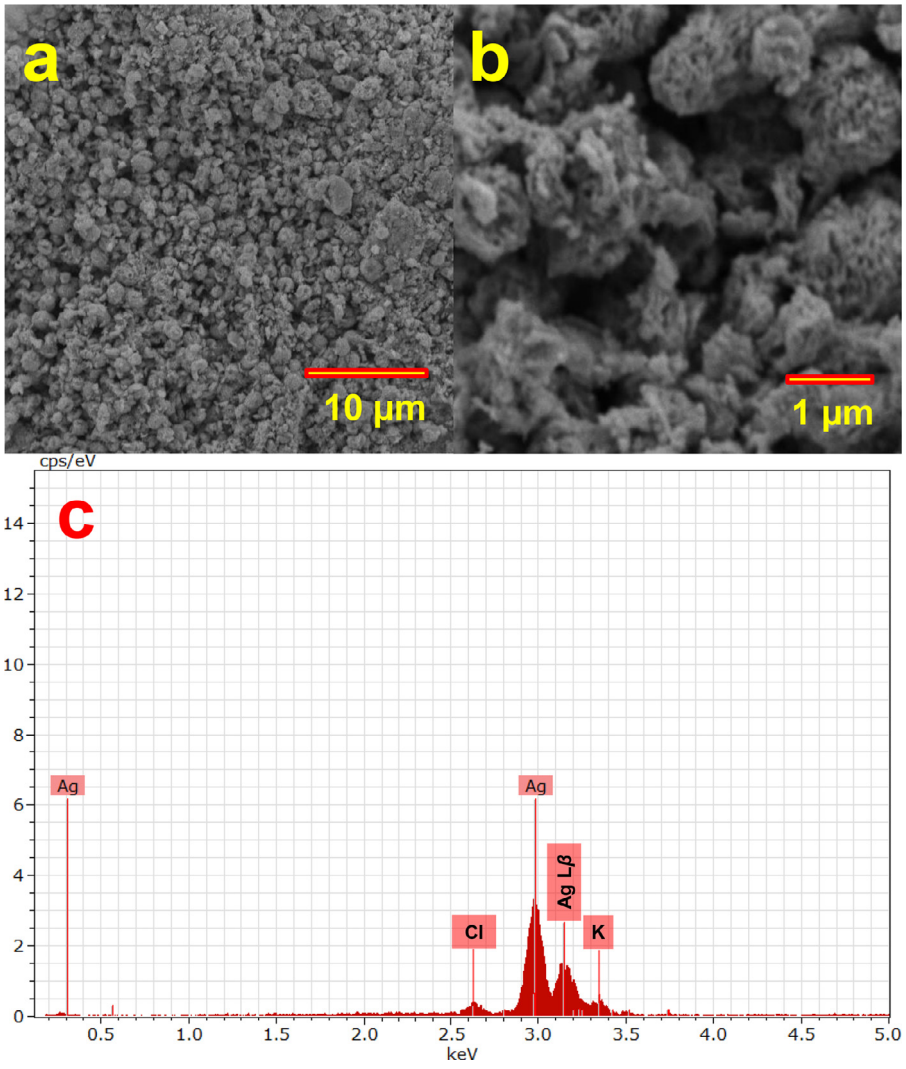

Fig. 6. **(a-c)** SEM with EDS spectrum of synthesized AS-AgNPs.

the valuable tools for the characterization of AgNPs. Fig. 2 (a, b) shows the UV-Vis spectra of silver precursor ($AgNO_3$), *A. scholaris* fruit extract and its AS-AgNPs synthesized using different concentrations of *A. scholaris* fruit extract. The Ag^+ ions display a strong absorbance peak at 264 nm in the UV region. Though the *A. scholaris* fruit extract shows two broad humps around 260 and 350 nm, respective to the $\pi-\pi^*$ and $n-\pi^*$ transition of alkaloidal constituents present in the fruit. In contrast, the synthesized AS-AgNPs show a clear and sharp SPR peak at 426 nm with a small hump at 350 nm, which suggest that AS-AgNPs are highly stable and protected by the phytoconstituents from aggregation [25]. It is noted that the absorbance intensity of AS-AgNPs is gradually increased while increasing the concentration of *A. scholaris* fruit which revealed that the formation rate of AS-AgNPs is higher at 5 mL of extract. Thus, the AS-AgNPs synthesized by 5 mL of the extract has been used for further characterization and application.

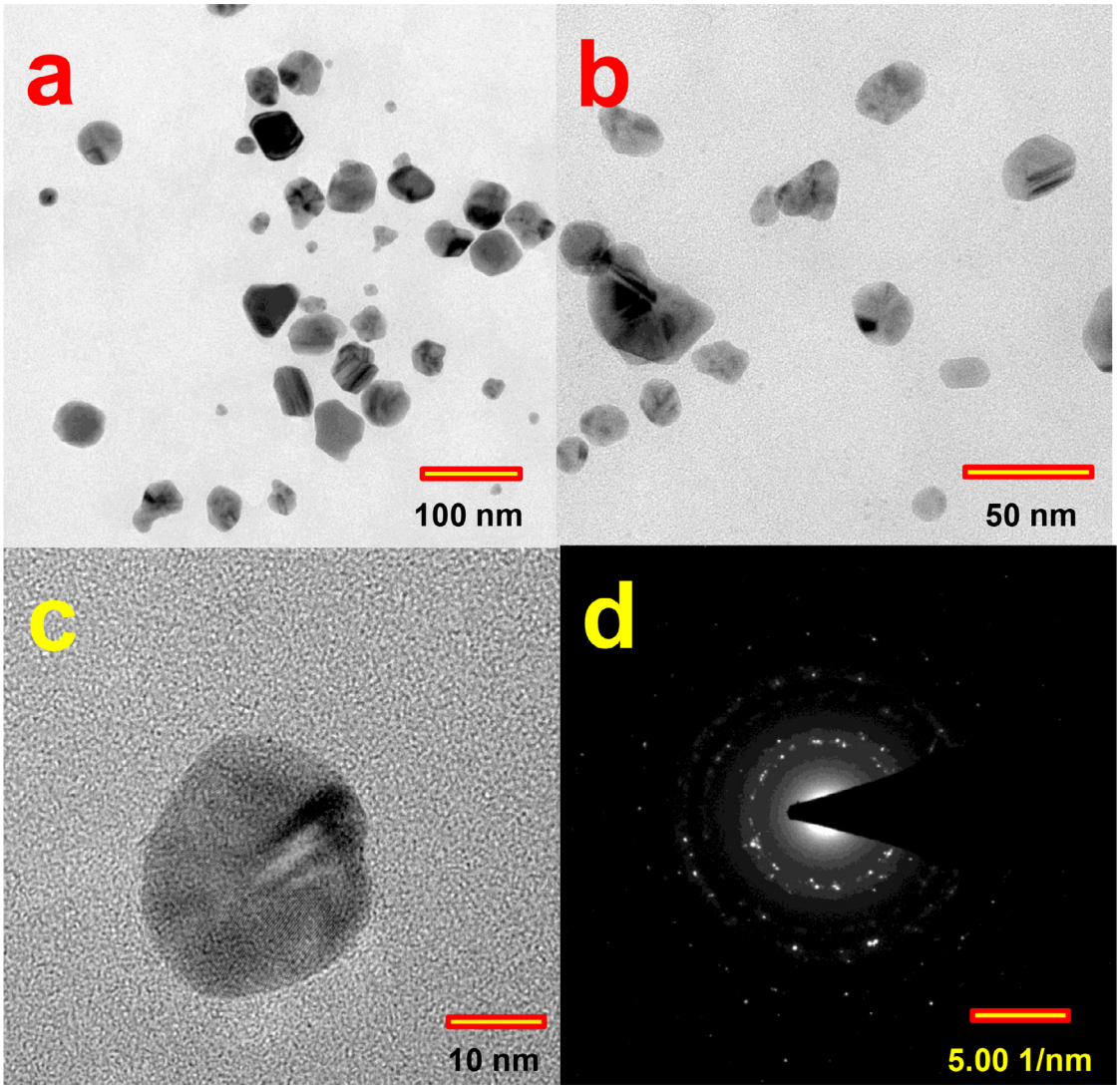

Fig. 7. **(a-d)** HR-TEM images and SAED pattern of AS-AgNPs.

3.2. FT-IR spectroscopy

The FT-IR spectroscopy is used to identify the responsible functional groups in the formation and protection of AS-AgNPs. The major phytochemicals present in the *A.scholaris* fruit are monoterpenoid indole alkaloids and aldehydes. Fig. 3 displays the FT-IR spectrum of dried AS-AgNPs, which shows a major band at 3419 cm^{-1} derived from the stretching vibrations of the N–H group present in the alkaloids. The asymmetric vibration of the methylene group is observed at 2914 cm^{-1}. The sharp absorption bands at 1578, 1385, and 1071 cm^{-1} correspond to N–H bending, C–N stretching and C–O stretching vibrations, respectively, which are attributed to the alkaloidal and carbonyl functionalities present in the extract. The small band at 695 cm^{-1} is attributed to the bending vibrations of –C–H groups [26–28]. As a result, the FT-IR spectrum of AS-AgNPs strongly propose that the phytoconstituents of *A.scholaris* fruit are mainly involved in the reduction of Ag^{+} ions and protection of AgNPs.

3.3. XRD

The crystal structure and crystallite size of AS-AgNPs are accessed through the XRD analysis. Fig. 4 represents the XRD pattern of AS-AgNPs. The sharp XRD peaks demonstrate a crystalline character of AS-AgNPs. Further, the XRD of AS-AgNPs shows four major diffraction peaks of the scattered 2θ angles at 38.2, 44.4, 64.7, and 77.4, which correspond to (111), (200), (220), and (311) lattice planes of the face-centered cubic structure of crystalline AgNPs [29–32]. The obtained pattern has highly resembled the crystalline silver and JCPDS file No. 087-0717 [33–34]. The crystallite size of AS-AgNPs is calculated to be 17 nm using Debye–Scherrer's equation, which is in good agreement with the HR-TEM results.

3.4. DLS and Zeta potential analysis

The investigation of scattered light obtained from the interaction of monochromatic light with AgNPs gives information related to particle size and dispersive nature. The DLS size distribution and zeta potential spectra of AS-AgNPs are presented in Fig. 5 (a, b). The calculated average particle size and poly dispersion index (PDI) of AS-AgNPs are about 50 nm and 0.664, respectively. The PDI value of AS-AgNPs falls in the range between 0 and 1, revealing the good stability of AS-AgNPs with mixed (mono and poly) dispersive nature [35–36]. Further, the obtained zeta potential of AS-AgNPs is -22.4 mV, suggested good stability [37]. The negative zeta potential of AS-AgNPs is mainly attributed to the capping of active phytoconstituents of *A.scholaris* fruit extract.

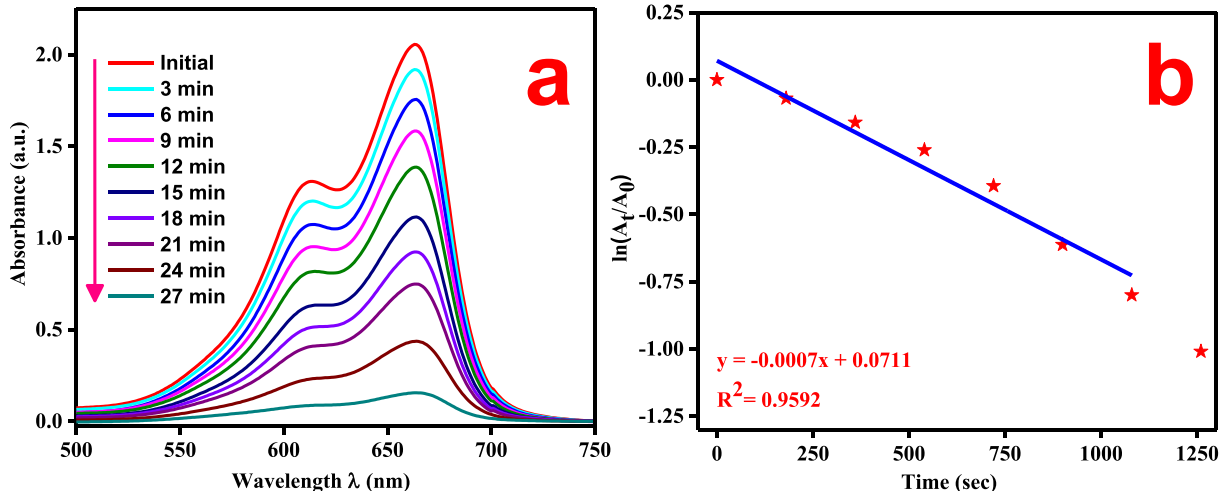

Fig. 8. a) UV-Vis spectra for the degradation of MB using $NaBH_4$ and AS-AgNPs; **b)** Pseudo first order kinetic plot for the degradation of MB.

3.5. SEM with EDS and HR-TEM analysis

Fig. 6 (a-c) depicts the SEM images with EDS spectrum of AS-AgNPs. The SEM images shows cluster-like spherical morphology of AS-AgNPs. Further, the EDS spectrum shows major peaks that appeared at 2.62, 2.93, 3.15 and 3.31 keV which are derived from Cl (Kα), Ag (Lα), Ag (Lβ) and K (Kα) elements present in the AS-AgNPs, where Cl and K elements may be originate from the plant pytoconstituents. The HR-TEM images and SAED pattern of AS-AgNPs are shown in Fig. 7(a-d). It is noticed that the AS-AgNPs are mainly distributed as a quasi-spherical shape with sizes ranging from 5 to 50 nm. In addition to that, some polyhedron shaped AgNPs could also be seen in the images. Based on the TEM images, the calculated percentages of quasi-spherical and polyhedron shaped AgNPs are as 56 and 44 %, respectively. Further, the presence of white dots in the SAED pattern of AS-AgNPs reveals the crystalline nature, which is mainly distributed in the (111) plane. All the results suggested that formation and good stability of synthesized AS-AgNPs. The major phytoconstituents present in the *A. scholaris* are monoterpenoid indole alkaloids and aldehydes, which are responsible for the reduction and protection of Ag^+ and AgNPs. The formation and aggregation properties of AgNPs are mainly connected to the structural and electronic properties of phytoconstituents, hence the large size distribution of AS-AgNPs may be attributed to the availability and involvement of various phytochemicals present in the *A. scholaris* fruit extract [38].

3.6. Catalytic degradation of MB

To show the practical application, the catalytic activity of AS-AgNPs is examined towards the degradation of MB by aqueous $NaBH_4$ using UV-Vis spectroscopy. MB is strongly absorbed at 664 nm in the visible region and yields deep blue color with the addition of aqueous $NaBH_4$. The reduction reaction of MB does not commence after the addition of $NaBH_4$, identified from the constant absorbance of MB. The reduction reaction begins after the addition of AS-AgNPs, which suggests that the synthesized AS-AgNPs act as a catalyst in the MB degradation. The time-dependent UV-Vis spectra of MB reduction are depicted in Fig. 8a. It is obvious that the absorbance intensity of MB gradually degrades and completes at 27 min with the brisk effervescence of H_2 gas. The calculated % degradation of MB is about 97 %. Further, the degradation kinetics of MB by $NaBH_4$ in the presence of AS-AgNPs is studied by pseudo first-order kinetics, the corresponding rate constant has been calculated using the following Eq. (1)

$$\ln\left[\frac{At}{A0}\right] = -kt \quad (1)$$

where A_0 is the initial absorbance intensity of MB, A_t is the absorbance intensity of MB at a time t and k is the rate constant [39]. Fig. 8b shows the pseudo first-order kinetics plot for the degradation of MB by aqueous $NaBH_4$ catalytically assisted by AS-AgNPs. It is noticed that time and $\ln(A_t/A_0)$ are linearly correlated and the resultant linearity coefficient value (R^2) is 0.9592 with a rate constant of 0.7×10^{-3} s^{-1}. The obtained rate constant value is comparatively higher than that of other catalysts reported in the literature [40–43]. The reductive degradation of MB can be explained by Langmuir-Hinshelwood (L-H) model proposed by many researchers [44]. According to the L-H model, $NaBH_4$ acts as an electron donor and hydrogen producer. After the addition of AS-AgNPs, concomitant adsorption of BH_4^- ions and MB occurred on the catalytic surface. Further, AS-AgNPs enable the degradation by acting electron transfer mediator between BH_4^- ions and MB, which leads to the potential degradation of MB.

4. Conclusion

This paper describes a simple, economic and eco-friendly approach for the synthesis of AgNPs using aqueous fruit extract of *A. scholaris*. The synthesized AS-AgNPs are absorbed at 426 nm in the visible region and looking brown color. The FT-IR of AS-AgNPs suggest that alkaloidal phytoconstituents of *A. scholaris* served as reducing and capping agents. The AS-AgNPs are crystalline with fcc geometrical arrangement, revealed by XRD. The size ranges of AS-AgNPs are calculated as 5 to 50 nm identified from the results of DLS and SEM. The negative Zeta potential value of AS-AgNPs (-22.4 mV) revealed their good stability. The shape of the AS-AgNPs is mainly quasi-spherical (56 %), which is exposed by HR-TEM images. Further, UV-Vis degradation results confirm the enhanced catalytic activity of AS-AgNPs on the degradation of MB by $NaBH_4$ and the calculated degradation rate constant is 0.7×10^{-3} s^{-1}. Thus, the green synthesized AS-AgNPs can be used as a catalyst for the degradation of toxic dyes.

Declaration of Competing Interest

On behalf of all authors, the corresponding author states that there is no conflict of interest.

CRediT authorship contribution statement

Rajamanickam Rajasekar: Conceptualization, Data curation, Writing – original draft. **Michael Samuel:** Methodology, Investigation, Software. **Thomas Nesakumar Jebakumar Immanuel Edison:** Writing – review & editing, Visualization, Validation, Formal analysis. **Natarajan Raman:** Validation, Supervision.

Acknowledgments

We express our sincere gratitude to the Principal, Head of the Chemistry Department, and College Managing Board members for providing the research facilities and constant encouragement.

References

[1] J. Nam, N. Won, H. Jin, H. Chung, S. Kim, pH-induced aggregation of gold nanoparticles for photothermal cancer therapy, J. Am. Chem. Soc. 131 (38) (2009) 13639–13645.
[2] K.B. Narayanan, N. Sakthivel, Synthesis and characterization of nano-gold composite using Cylindrocladium floridanum and its heterogeneous catalysis in the degradation of 4-nitrophenol, J. Hazard. Mater. 189 (1–2) (2011) 519–525.
[3] J. Li, X. Chen, N. Ai, J. Hao, Q. Chen, S. Strauf, Y. Shi, Silver nanoparticle doped TiO2 nanofiber dye sensitized solar cells, Chem. Phys. Lett. 514 (1–3) (2011) 141–145.
[4] A.M. Fayaz, M. Girilal, S.A. Mahdy, S.S. Somsundar, R. Venkatesan, P.T. Kalaichelvan, Vancomycin bound biogenic gold nanoparticles: a different perspective for development of anti VRSA agents, Process Biochem. 46 (3) (2011) 636–641.
[5] P. Sutradhar, M. Saha, AgNPs: synthesis and its nanocomposites for heterojunction polymer solar cells, J. Phys. Chem. C 120 (16) (2016) 8941–8949.
[6] N. Tarannum, Gauta.m Y.K. Divya, Facile green synthesis and applications of silver nanoparticles: a state-of-the-art review, RSC Adv. 9 (2019) 34926–34948.
[7] J. Bahadur, S. Agrawal, V. Panwar, A. Parveen, K. Pal, Antibacterial properties of silver doped TiO2 nanoparticles synthesized via sol-gel technique, Macromol. Res. 24 (6) (2016) 488–493.
[8] D.O. Oseguera-Galindo, R. Machorro-Mejia, N. Bogdanchikova, J.D. Mota–Morales, AgNPs synthesized by laser ablation confined in urea choline chloride deep-eutectic solvent, Colloid Interface Sci. Commun. 12 (2016) 1–4.
[9] M.T. Yaraki, M. Tayebi, M. Ahmadieh, M. Tahriri, D. Vashaee, L. Tayebi, Synthesis and optical properties of cysteamine-capped ZnS quantum dots for aflatoxin quantification, J. Alloys Compd. 690 (2017) 749–758.
[10] M. Tayebi, M.T. Yaraki, M. Ahmadieh, A. Mogharei, M. Tahriri, D. Vashaee, L. Tayebi, Synthesis, surface modification and optical properties of thioglycolic acid-capped ZnS quantum dots for starch recognition at ultralow concentration, J. Electron. Mater. 45 (11) (2016) 5671–5678.
[11] M. Tayebi, M.T. Yaraki, M. Ahmadieh, M. Tahriri, D. Vashaee, L. Tayebi, Determination of total aflatoxin using cysteamine-capped CdS quantum dots as a fluorescence probe, Colloid Polym. Sci. 294 (9) (2016) 1453–1462.
[12] M.V. Gorbachevskiy, D.S. Kopitsyn, I.A. Tiunov, M.S. Kotelev, V.A. Vinokurov, A.A. Novikov, Synthesis of bimetallic gold/AgNPs via in situ seeding, Russ. J. Phys. Chem. A 91 (1) (2017) 141–144.
[13] Y.Y. Jhuang, W.T. Cheng, Fabrication and characterization of silver/titanium dioxide composite nanoparticles in ethylene glycol with alkaline solution through sonochemical process, Ultrason. Sonochem. 28 (2016) 327–333.
[14] C. Dong, F. Cheng, X. Zhang, X. Wang, X. Xiao, C. Cao, B. Yuan, Facile synthesis and characterization of monodisperse silver colloidal nanoparticles stabilized by sodium laurate, Iranian J. Sci. Technol., Trans. A 42 (4) (2018) 1905–1913.
[15] P.S. Thomas, A. Kanaujia, D. Ghosh, R. Duggar, C.K. Katiyar, Alstonoside, a secoiridoid glucoside from Alstonia scholaris, Indian J. Chem. 47B (2008) 1298–1302.
[16] N. G Shimpi, S. Shirole, S. Mishra, Biogenesis synthesis and characterization of AgNPs (AgNPs) using the aqueous extract of Alstonia scholaris: a greener approach, Micro Nanosyst. 7 (1) (2015) 49–54.
[17] Y.L. Zhao, S.B. Pu, Y. Qi, B.F. Wu, J.H. Shang, Y.P. Liu, X.D. Luo, Pharmacological effects of indole alkaloids from Alstonia scholaris (L.) R. Br. on pulmonary fibrosis in vivo, J. Ethnopharmacol. 267 (2021) 113506.
[18] S. Saroj, K. Kumar, N. Pareek, R. Prasad, R.P. Singh, Biodegradation of azo dyes Acid Red 183, Direct Blue 15 and Direct Red 75 by the isolate Penicillium oxalicum SAR-3, Chemosphere 107 (2014) 240–248.
[19] J. Feng, C.E. Cerniglia, H. Chen, Toxicological significance of azo dye metabolism by human intestinal microbiota, Front. Biosci. (Elite edition) 4 (2012) 568.
[20] J. Fito, S. Abrham, K. Angassa, Adsorption of methylene blue from textile industrial wastewater onto activated carbon of Parthenium hysterophorus, Int. J. Environ. Res. 14 (5) (2020) 501–511.
[21] D. Hebbalalu, J. Lalley, M.N. Nadagouda, R.S. Varma, Greener techniques for the synthesis of AgNPs using plant extracts, enzymes, bacteria, biodegradable polymers, and microwaves, ACS Sustain. Chem. Eng. 1 (7) (2013) 703–712.
[22] K.R. Aadil, N. Pandey, S.I. Mussatto, H. Jha, Green synthesis of AgNPs using acacia lignin, their cytotoxicity, catalytic, metal ion sensing capability and antibacterial activity, J. Environ. Chem. Eng. 7 (5) (2019) 103296.
[23] J. Singh, A. Mehta, M. Rawat, S. Basu, Green synthesis of AgNPs using sun dried tulsi leaves and its catalytic application for 4-Nitrophenol reduction, J. Environ. Chem. Eng. 6 (1) (2018) 1468–1474.
[24] M. Aravind, A. Ahmad, I. Ahmad, M. Amalanathan, K. Naseem, S.M.M. Mary, M. Zuber, Critical green routing synthesis of silver NPs using jasmine flower extract for biological activities and photocatalytical degradation of methylene blue, J. Environ. Chem. Eng. 9 (1) (2021) 104877.
[25] V. Morales-Lozoya, H. Espinoza-Gómez, L.Z. Flores-López, E.L. Sotelo-Barrera, A. Núñez-Rivera, R.D. Cadena-Nava, I.A. Rivero, Study of the effect of the different parts of Morinda citrifolia L.(noni) on the green synthesis of AgNPs and their antibacterial activity, Appl. Surf. Sci. 537 (2021) 147855.
[26] I. Fatimah, Green synthesis of AgNPs using extract of Parkia speciosa Hassk pods assisted by microwave irradiation, J. Adv. Res. 7 (6) (2016) 961–969.
[27] G. Bagherzade, M.M. Tavakoli, M.H. Namaei, Green synthesis of AgNPs using aqueous extract of saffron (Crocus sativus L.) wastages and its antibacterial activity against six bacteria, Asian Pac. J. Trop. Biomed. 7 (3) (2017) 227–233.
[28] H. Padalia, P. Moteriya, S. Chanda, Green synthesis of AgNPs from marigold flower and its synergistic antimicrobial potential, Arabian J. Chem. 8 (5) (2015) 732–741.
[29] V. Dhand, L. Soumya, S. Bharadwaj, S. Chakra, D. Bhatt, B. Sreedhar, Green synthesis of AgNPs using Coffea arabica seed extract and its antibacterial activity, Mater. Sci. Eng. 58 (2016) 36–43.
[30] N.H. Rao, N. Lakshmidevi, S.V.N. Pammi, P. Kollu, S. Ganapaty, P. Lakshmi, Green synthesis of AgNPs using methanolic root extracts of Diospyros paniculata and their antimicrobial activities, Mater. Sci. Eng. 62 (2016) 553–557.
[31] J.L. López-Miranda, M. Vázquez, N. Fletes, R. Esparza, G. Rosas, Biosynthesis of AgNPs using a Tamarix gallica leaf extract and their antibacterial activity, Mater. Lett. 176 (2016) 285–289.
[32] V. Ravichandran, S. Vasanthi, S. Shalini, S.A.A. Shah, R. Harish, Green synthesis of AgNPs using Atrocarpus altilis leaf extract and the study of their antimicrobial and antioxidant activity, Mater. Lett. 180 (2016) 264–267.
[33] M.J. Ahmed, G. Murtaza, A. Mehmood, T.M. Bhatti, Green synthesis of AgNPs using leaves extract of Skimmia laureola: characterization and antibacterial activity, Mater. Lett. 153 (2015) 10–13.
[34] T.N.J.I. Edison, Y.R. Lee, M.G. Sethuraman, Green synthesis of AgNPs using Terminalia cuneata and its catalytic action in reduction of direct yellow-12 dye, Spectrochim. Acta Part A 161 (2016) 122–129.
[35] A. Venkatalaxmi, B.S. Padmavathi, T. Amaranath, A general solution of unsteady Stokes equations, Fluid Dyn. Res. 35 (3) (2004) 229–236.
[36] K. Shameli, M. Bin Ahmad, E.A. Jaffar Al-Mulla, N.A. Ibrahim, P. Shabanzadeh, A. Rustaiyan, M. Zidan, Green biosynthesis of AgNPs using Callicarpa maingayi stem bark extraction, Molecules 17 (7) (2012) 8506–8517.
[37] S. Ahmed, M. Ahmad, B.L. Swami, S. Ikram, A review on plants extract mediated synthesis of AgNPs for antimicrobial applications: a green expertise, J. Adv. Res. 7 (1) (2016) 17–28.
[38] A. Salayova, Z. Bedlovicova, N. Daneu, M. Balaz, Z.L. Bujnakova, L. Balazova, L. Tkacikova, Green synthesis of silver nanoparticles with antibacterial activity using various medicinal plant extracts: morphology and antibacterial efficacy, Nanomaterials 11 (4) (2021) 1005 (DOI: 10.3390/nano11041005).
[39] M. Ider, K. Abderrafi, A. Eddahbi, S. Ouaskit, A. Kassiba, Silver metallic nanoparticles with surface plasmon resonance: synthesis and characterizations, J. Cluster Sci. 28 (3) (2017) 1051–1069.
[40] K.B.A. Ahmed, R. Senthilnathan, S. Megarajan, V. Anbazhagan, Sunlight mediated synthesis of AgNPs using redox phytoprotein and their application in catalysis and colorimetric mercury sensing, J. Photochem. Photobiol. B 151 (2015) 39–45.
[41] X. Wei, M. Luo, W. Li, L. Yang, X. Liang, L. Xu, H. Liu, Synthesis of AgNPs by solar irradiation of cell-free Bacillus amyloliquefaciens extracts and $AgNO_3$, Bioresour. Technol. 103 (1) (2012) 273–278.
[42] L. Sherin, A. Sohail, M. Mustafa, R. Jabeen, A. Ul-Hamid, Facile green synthesis of AgNPs using Terminalia bellerica kernel extract for catalytic reduction of anthropogenic water pollutants, Colloid Interface Sci. Commun. 37 (2020) 100276.
[43] A.A. Mashentseva, M. Barsbay, N.A. Aimanova, M.V. Zdorovets, Application of silver-loaded composite track-etched membranes for photocatalytic decomposition of methylene blue under visible light, Membranes 11 (1) (2021) 60.
[44] K. Naseem, M. Zia Ur Rehman, A. Ahmad, D. Dubal, T.S. AlGarni, Plant extract induced biogenic preparation of silver nanoparticles and their potential as catalyst for degradation of toxic dyes, Coatings 10 (12) (2020) 1235.